Chinese Journal of Aeronautics, (2019), 32(4): 938–947

Chinese Society of Aeronautics and Astronautics
& Beihang University

Chinese Journal of Aeronautics

cja@buaa.edu.cn
www.sciencedirect.com

Constitutive modelling of composite laminates under uniaxial compression

Hsuan-Teh HU *, **Lung-Shen KE**

Department of Civil Engineering, "National" Cheng Kung University, Tainan 701, China

Received 6 February 2018; revised 28 June 2018; accepted 8 November 2018
Available online 14 February 2019

KEYWORDS

Composite laminates;
Constitutive model;
Finite element analysis;
Nonlinearity;
Uniaxial compression

Abstract A nonlinear constitutive model for a single lamina is proposed for the failure analysis of composite laminates. In the material model, both fiber and matrix are assumed to behave elastic-plastically and the in-plane shear is assumed to behave nonlinearly with a variable shear parameter. The damage onset for individual lamina is detected by a mixed failure criterion, composed of the Tsai-Wu criterion and the maximum stress criterion. After damage takes place within the lamina, the fiber and in-plane shear are assumed to exhibit brittle behavior, and the matrix is assumed to exhibit degrading behavior. The proposed nonlinear material model is tested against experimental data of composite laminates subjected to uniaxial compressive loads, and good agreement is obtained.

1. Introduction

Due to lightweight and high strength, the use of composite laminate materials in aerospace industry has increased rapidly in recent years. Numerous cases involving the design of composite structures show that there is a need for more refined analysis that takes into account phenomena such as progressive failure and inelastic or nonlinear deformation of composite materials.[1–12] It is well known that unidirectional fibrous composites exhibit severe nonlinearity in their in-plane shear stress-strain relations.[13] In addition, deviation from linearity is also observed with in-plane transverse loading but the degree of nonlinearity is not comparable to that observed with the in-plane shear.[14,15] Therefore, appropriate modeling of the nonlinear behavior of fiber-reinforced composite materials becomes crucial.

A significant number of macro-mechanical models have been proposed to represent the constitutive relation of fiber-reinforced composite materials such as nonlinear elasticity models,[13,14,16] plasticity models,[17–19] or damage theory coupled with elasticity.[20] In addition, various failure criteria have also been proposed to predict the onset of damage in single layers within fiber-reinforced composites, i.e., limit theories,[21] polynomial theories,[22,23] and direct mode-determining theories.[24–27] As for the post-damage process of individual lamina, two idealized types of failure modes have been defined in a previous study;[19] namely, brittle mode and ductile mode. In the case of the brittle mode, the material gives up its entire stiffness and strength in the dominant stress direction as the damage is

* Corresponding author.
E-mail address: hthu@mail.ncku.edu.tw (H.-T. HU).

Peer review under responsibility of Editorial Committee of CJA.

Production and hosting by Elsevier

https://doi.org/10.1016/j.cja.2019.02.003

reached. For the ductile mode, the material retains its strength but loses its overall stiffness in the direction of damage.

Obviously, a rational analysis of the individual layers within the laminate under loading must include three parts, i.e., pre-damage analysis, damage onset determination, and post-damage analysis. In the pre-damage analysis, the proper constitutive model of lamina is a key tool to describe the real behavior of each layer within the laminate under loading. In previous studies, it is assumed that the fiber and matrix perform with elastic-plastic behavior,[19] and the in-plane shear behaves nonlinearly with a constant shear parameter.[25] In this study, it is proposed that the in-plane shear behaves nonlinearly with a variable shear parameter. The difference between these two distinct types of shear parameters is investigated in this study. Up to now, the Tsai-Wu failure criterion[8,23] is the most common criterion used to determine the damage onset of individual layer. However, Hu et al.[28–30] point out that the Tsai-Wu failure criterion would cause overestimated failure stresses in the fiber direction of the composite lamina. To eliminate this unreasonable phenomenon, an extra limitation should be added into the Tsai-Wu failure criterion to obtain a more accurate and reasonable stresses in the composite lamina. As the results, Zhu and Sankar[31] and Hu et al. [28–30] suggested that the combination of both the Tsai-Wu criterion and the maximum stress criterion, which is called the mixed criterion, was a much better criterion for determining the damage to lamina. Thus, in this paper, a mixed criterion is employed to determine the damage onset of individual layers. For the post-damage analysis, a degrading mode for matrix and brittle modes for fiber and in-plane shear are proposed to simulate the post damage behavior of individual lamina.

In this paper, the proposed nonlinear analysis model is developed first. Then, various failure criteria and post damage modes are reviewed, and a mixed failure criterion and the post-damage modes are proposed. Finally, the ABAQUS finite element program[32] is used to verify the proposed constitutive model against experimental data of Petit and Waddoups[14] and the conclusions obtained from the numerical analysis are given.

2. Nonlinear analysis model

2.1. Proposed stress-strain curves and post damage models

Fig. 1 shows the material, element and structure coordinates of fiber reinforced plastics. In Fig. 1, (1, 2, 3) means the material coordinate, where 1 indicates the fiber direction, 2 indicates the orthogonal direction to the fiber direction in the plane of the lamina, and 3 refers the transverse direction to the plane of the lamina. In addition, (x, y, z) represents the element local coordinate system, and (X, Y, Z) the structural global coordinate system.

For a single lamina subjected to tensile loading, the stress-strain curves of the nonlinear analysis model are shown in Figs. 2(a) and (b). It is assumed that the material response can be represented by elastic-plastic stress-strain curves in the principal material directions, i.e., the 1 direction (fiber direction) and the 2 direction (transverse direction), of the lamina. Let X_{yt} and X_{ut} be the yield strength and the ultimate strength of the lamina for tension in the 1 direction, Y_{yt} and Y_{ut} be the yield strength and the ultimate strength of the lamina for tension in the 2 direction. For the elastic regions, i.e., $\sigma_1 \leqslant X_{yt}$ and $\sigma_2 \leqslant Y_{yt}$, the elastic moduli are denoted by E_{iie} ($i = 1, 2$). For the plastic regions, i.e., $X_{yt} \leqslant \sigma_1 \leqslant X_{ut}$ and $Y_{yt} \leqslant \sigma_2 \leqslant Y_{ut}$, the elastic moduli are denoted by E_{iipt} ($i = 1, 2$). For a lamina subjected to compressive loading, the stress-strain curves are shown in Figs. 2(c) and (d). It is obvious that X_{yc} and X_{uc} are the yield strength and the ultimate strength of the lamina for compression in the 1 direction and that Y_{yc} and Y_{uc} are the yield strength and the ultimate strength of the lamina for compression in the 2 direction. For the plastic regions, i.e., $X_{yc} \leqslant \sigma_1 \leqslant X_{uc}$ and $Y_{yc} \leqslant \sigma_2 \leqslant Y_{uc}$, the elastic moduli are denoted by E_{iipc} ($i = 1, 2$). Let S be the ultimate in-plane shear strength. It is assumed that the in-plane shear in the 1-2 direction can be modeled by a nonlinear stress-strain curve as shown in Fig. 2(e).

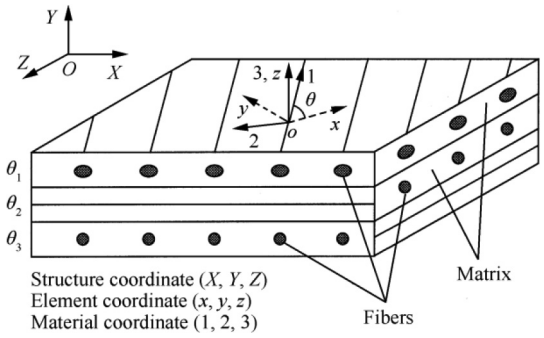

Fig. 1 Material, element and structure coordinates of fiber reinforced plastics.

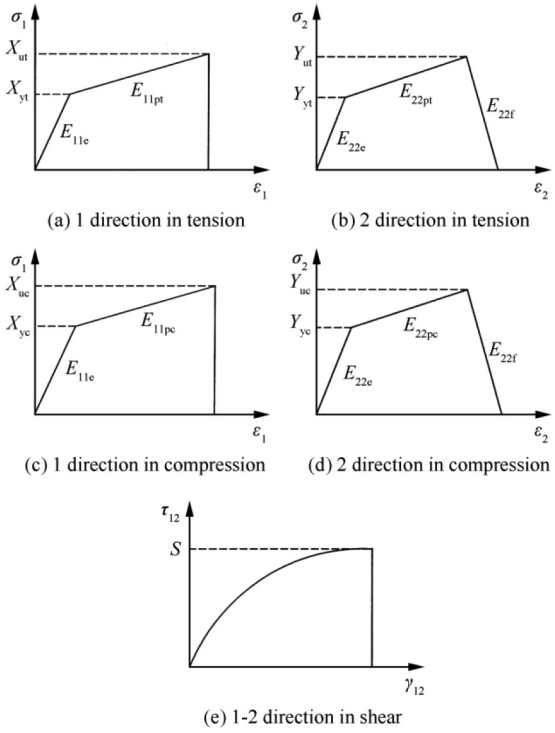

Fig. 2 Stress-strain curves of the proposed nonlinear failure model.

For the post-damage region, the strengths of the lamina are dropped to zero (brittle modes) in the 1 direction (Figs. 2(a) and (c)) and the 1-2 direction (Fig. 2(e)). This is because the failures of the lamina in 1 and 1-2 directions are dominated by fiber and its failure mode is sudden and brittle. It is known that the failure of the lamina in the 2 direction is dominated by matrix. After the failure of the matrix occurs, its strength would drop to zero gradually. Hence, in the proposed model the elastic stiffness of the lamina is assumed to have a negative modulus E_{22f} in the 2 direction (degrading mode) and the damaged lamina unloads in the transverse direction until no stress remains in the lamina (Figs. 2(b) and (d)).

2.2. Nonlinear constitutive model of the lamina

For fiber-composite laminate materials, each lamina can be considered to be an orthotropic layer in a plane stress condition. Taking into account the elastic-plastic behavior in the 1 and 2 directions and the nonlinear behavior on the 1-2 plane within the lamina, the strain-stress relations for an orthotropic lamina in the material coordinates (1,2) can be written as[13]

$$\begin{bmatrix}\varepsilon_1\\ \varepsilon_2\\ \gamma_{12}\end{bmatrix}=\begin{bmatrix}\frac{1}{E_{11}} & \frac{-\upsilon_{21}}{E_{22}} & 0\\ \frac{-\upsilon_{12}}{E_{11}} & \frac{1}{E_{22}} & 0\\ 0 & 0 & \frac{1}{G_{12}}\end{bmatrix}\begin{bmatrix}\sigma_1\\ \sigma_2\\ \tau_{12}\end{bmatrix}+S_{66}\tau_{12}^2\begin{bmatrix}0\\ 0\\ \tau_{12}\end{bmatrix} \tag{1}$$

where ε_1, ε_2, and γ_{12} represent the strains in the 1 direction, 2 direction and the 1-2 plane, respectively. The σ_1, σ_2 and τ_{12} denote the stresses in the 1 direction, 2 direction and the 1-2 plane, respectively. The υ_{12} and υ_{21} are Poisson's ratios, and E_{11} and E_{22} are the elastic moduli in the 1 and 2 directions. If the lamina is in the elastic stage in the 1 or 2 direction, then $E_{11} = E_{11e}$ or $E_{22} = E_{22e}$. If the lamina is in the plastic stage in the 1 or 2 direction, then $E_{11} = E_{11p}$ or $E_{22} = E_{22p}$. The G_{12} is the shear modulus, and S_{66} is a shear parameter to account for the in-plane shear nonlinearity. The S_{66} shear parameter in Eq. (1) was derived by Hahn and Tsai[13] using the complementary elastic energy density and has been verified against the experimental data on off-axis tests. For a specific composite lamina, the value of S_{66} can be determined by a curve fit to pure shear test data.

The incremental stress-strain relations for a nonlinear orthotropic lamina can be given as follows:

$$\Delta\boldsymbol{\sigma}' = \boldsymbol{Q}_1'\Delta\boldsymbol{\varepsilon}' \tag{2}$$

$$\Delta\boldsymbol{\tau}_t' = \boldsymbol{Q}_2'\Delta\boldsymbol{\gamma}_t' \tag{3}$$

where $\Delta\boldsymbol{\sigma}' = [\Delta\sigma_1, \Delta\sigma_2, \Delta\tau_{12}]^T$, $\Delta\boldsymbol{\tau}_t' = [\Delta\tau_{13}, \Delta\tau_{23}]^T$, $\Delta\boldsymbol{\varepsilon}' = [\Delta\varepsilon_1, \Delta\varepsilon_2, \Delta\gamma_{12}]^T$, $\Delta\boldsymbol{\gamma}_t' = [\Delta\gamma_{13}, \Delta\gamma_{23}]^T$ and

$$\boldsymbol{Q}_1' = \begin{bmatrix}\frac{E_{11}}{1-\upsilon_{12}\upsilon_{21}} & \frac{\upsilon_{12}E_{22}}{1-\upsilon_{12}\upsilon_{21}} & 0\\ \frac{\upsilon_{21}E_{11}}{1-\upsilon_{12}\upsilon_{21}} & \frac{E_{22}}{1-\upsilon_{12}\upsilon_{21}} & 0\\ 0 & 0 & \frac{1}{1/G_{12}+3S_{66}\tau_{12}^2}\end{bmatrix} \tag{4}$$

$$\boldsymbol{Q}_2' = \begin{bmatrix}\alpha_1 G_{13} & 0\\ 0 & \alpha_2 G_{23}\end{bmatrix} \tag{5}$$

The terms α_1 and α_2 are the shear correction factors and are taken to be 0.83 in this study.[33] It is assumed that the transverse shear stresses always behave linearly and do not affect the nonlinear in-plane behavior of individual lamina.

3. Failure criterion, degradation of stiffness and laminate governing equations

3.1. Review of failure criteria

As previously mentioned, failure criteria fall into three basic categories: (A) limit theories,[21] (B) polynomial theories,[22,23] and (C) direct mode determining theories.[24–27] Among them, the most popular criteria, i.e., the maximum stress criterion[21] and the Tsai-Wu failure criterion,[23] are selected to be briefly reviewed.

3.1.1. Maximum stress criterion

The maximum stress criterion is the dominant member of the limit failure theory category.[21] For the plane stress condition, the maximum stress criterion for an orthotropic material can be expressed as follows:

$$\frac{\sigma_1}{X_{ut}} = 1 \quad \text{or} \quad \frac{\sigma_1}{X_{uc}} = 1 \tag{6}$$

$$\frac{\sigma_2}{Y_{ut}} = 1 \quad \text{or} \quad \frac{\sigma_2}{Y_{uc}} = 1 \tag{7}$$

$$\frac{\tau_{12}}{S} = 1 \tag{8}$$

3.1.2. Tsai-Wu failure criterion

The Tsai-Wu failure criterion has a general nature, because it contains almost all other polynomial theories as special cases. Under the plane stress condition, the Tsai-Wu failure criterion has the following form:[23]

$$F_1\sigma_1 + F_2\sigma_2 + F_{11}\sigma_1^2 + 2F_{12}\sigma_1\sigma_2 + F_{22}\sigma_2^2 + F_{66}\tau_{12}^2 = 1 \tag{9a}$$

where

$$\begin{cases} F_1 = \frac{1}{X_{ut}} + \frac{1}{X_{uc}} \\ F_{11} = \frac{1}{X_{ut}X_{uc}} \\ F_2 = \frac{1}{Y_{ut}} + \frac{1}{Y_{uc}} \\ F_{22} = \frac{1}{Y_{ut}Y_{uc}} \\ F_{66} = \frac{1}{S^2} \end{cases} \tag{9b}$$

The stress interaction term F_{12} in Eq. (9a) is difficult to determine. In lieu of additional experimental data on other materials and loading conditions, a numerical experiment was performed by Narayanaswami and Adelman[34] to estimate the errors for ten different composite systems under six different loadings. The maximum error in predicted failure loads among all cases was below 10 percent. These results suggest that the Tsai-Wu failure criterion with $F_{12} = 0$ can predict failure of practical composite materials under general biaxial loading with sufficient accuracy for engineering applications. Thus, the use of Tsai-Wu failure criterion with $F_{12} = 0$ is recommended as a preferred alternative to the experimental determination of F_{12} for orthotropic laminae. As the result, $F_{12} = 0$ is used in this study.

3.2. Mixed failure criterion

Although the Tsai-Wu failure criterion is widely used in determining the damage onset of a lamina, there are some draw-

backs with it. Among them is the fact that the failure stress of fiber in a lamina may exceed the strength of the material in the case of symmetric angle-ply laminates with a small fiber angle (say $0^\circ < \theta < 20^\circ$) subjected to off-axis tension.[28,29] In order to eliminate this unreasonable phenomenon, the limitation of the maximum stress of the lamina in the fiber direction is added into the Tsai-Wu failure criterion to obtain a mixed failure criterion, which has the following formulations:

$$F_1\sigma_1 + F_2\sigma_2 + F_{11}\sigma_1^2 + F_{22}\sigma_2^2 + F_{66}\tau_{12}^2 = 1 \tag{10}$$

and

$$\frac{\sigma_1}{X_{ut}} \leqslant 1 \quad \text{or} \quad \frac{\sigma_1}{X_{uc}} \leqslant 1 \tag{11}$$

3.3. Normalized failure stresses and failure contribution

The Tsai-Wu failure criterion and the mixed failure criterion consider the coupling effect of in-plane stresses, σ_1, σ_2 and τ_{12}, in the lamina when the collapse occurs. In order to determine the individual stress ratio in the lamina, the normalized failure stresses are defined, which represent the stress ratios (failure stresses/corresponding strengths) in the lamina for various stresses at the onset of collapse. The expressions for the normalized failure stresses are described as follows:

$$(\sigma_{11f})_n = \frac{\sigma_{11f}}{X_{ut}} \quad \text{or} \quad (\sigma_{11f})_n = \frac{\sigma_{11f}}{|X_{uc}|} \tag{12a}$$

$$(\sigma_{22f})_n = \frac{\sigma_{22f}}{Y_{ut}} \quad \text{or} \quad (\sigma_{22f})_n = \frac{\sigma_{22f}}{|Y_{uc}|} \tag{12b}$$

$$(\tau_{12f})_n = \left|\frac{\tau_{12f}}{S}\right| \tag{12c}$$

where $(\sigma_{11f})_n$, $(\sigma_{22f})_n$ and $(\tau_{12f})_n$ denote the normalized failure stresses in the 1 direction, 2 direction, and the 1-2 plane of the lamina, respectively. The σ_{11f}, σ_{22f} and τ_{12f} are the stresses of the lamina in the 1 direction, 2 direction and the 1-2 plane at the onset of failure.

3.4. Proposed degradation models

Upon damage within the lamina occurring, the material properties begin to degrade. Material degradation within the damaged area is evaluated by the mode of failure predicted by the failure criterion. Therefore, the residual stiffness of composite strongly depends on the failure mode in each layer. According to the literature, the degradation models for each layer are categorized into three types of failure modes, i.e., the brittle mode, the ductile mode[19] and the degrading mode.[28–30] For the brittle mode, the material loses its entire stiffness and strength in the dominant stress direction. For the ductile mode, the material retains its strength but loses all of its stiffness in the failure direction. For the degrading mode, the material loses its stiffness and strength in the failure direction gradually until the stress in that direction is reduced to zero.

In this investigation, it is proposed that the post damage modes are the brittle behavior for σ_1 and τ_{12}, and the degrading behavior for σ_2 (Fig. 2). The following three rules are used to determine whether the ply failure is caused by matrix fracture, shear failure, or as a result of fiber breakage or buckling[35,36]:

(1) If a ply fails in the condition of $X_{uc} < \sigma_1 < X_{ut}$, and $-S < \tau_{12} < S$, the damage is assumed to be matrix induced. Consequently, the degradation of transverse stiffness occurs. Due to the interlock action with the neighboring plies, the damaged ply gradually loses its capability to support transverse stress, until the fracture in shear or the breakage or buckling in fiber on the same ply occurs. However, the lamina remains able to carry the longitudinal and shear stresses. In this case, the constitutive matrix of the lamina becomes

$$\boldsymbol{Q}_1' = \begin{bmatrix} E_{11} & 0 & 0 \\ 0 & E_{22f} & 0 \\ 0 & 0 & \frac{1}{1/G_{12}+3S_{66}\tau_{12}^2} \end{bmatrix} \tag{13}$$

where E_{22f} is a negative tangent modulus in the transverse direction of the lamina after matrix damage. In the proposed model, the shear parameter S_{66} has a variable value.

(2) If the ply fails in the condition of $X_{uc} < \sigma_1 < X_{ut}$, and $\tau_{12} \geqslant S$ or $\tau_{12} \leqslant -S$, the damage is assumed to be shear induced. Consequently, the damaged lamina loses its capability to support transverse and shear stresses, but remains able to carry longitudinal stress. In this case, the constitutive matrix of the lamina becomes

$$\boldsymbol{Q}_1' = \begin{bmatrix} E_{11} & 0 & 0 \\ 0 & 0 & 0 \\ 0 & 0 & 0 \end{bmatrix} \tag{14}$$

(3) If the ply fails with $\sigma_1 \geqslant X_{ut}$, or $\sigma_1 \geqslant X_{uc}$, the ply failure is caused by fiber breakage or buckling and a total ply rupture is assumed. Thus, the constitutive matrix of the lamina becomes

$$\boldsymbol{Q}_1' = \begin{bmatrix} 0 & 0 & 0 \\ 0 & 0 & 0 \\ 0 & 0 & 0 \end{bmatrix} \tag{15}$$

3.5. Laminate governing equations

The forgoing nonlinear failure analysis model for fiber-reinforced composite lamina can be combined with classical lamination theory to form the following incremental laminate force-strain relations: in-plane

$$\Delta \boldsymbol{N} = \sum_{i=1}^{n} \boldsymbol{Q}_i t_i \Delta\varepsilon \tag{16}$$

where $\Delta N = \left[\Delta N_x, \Delta N_y, \Delta N_{xy}\right]^T$ and $\Delta\boldsymbol{\varepsilon} = \left[\Delta\varepsilon_x, \Delta\varepsilon_y, \Delta\varepsilon_{xy}\right]^T$ are the vectors of the incremental in-plane forces and the incremental strains in the overall laminate coordinate system (x, y), respectively. The term t_i is the thickness of the i-th layer; n is the total number of layers. The matrix Q_i stands for constitutive matrix for the i-th layer and can be obtained by proper rotation of the Q_1' matrix of that layer.[36]

4. Numerical analysis

4.1. Numerical simulations and material properties

The aforementioned nonlinear constitutive model combined with various failure criteria and various post damage modes for composite materials are written in a FORTRAN subroutine, i.e., the user-defined material model, UMAT. Then this UMAT subroutine is linked to the ABAQUS finite element program[32] for the numerical analyses. The subroutine will be called at all material calculation points of elements for which the material definition includes a user-defined material behavior. The ABAQUS program will pass the previous strains and the current incremental strains to the UMAT subroutine. The subroutine must update the stresses and solution-dependent state variables to their values at the end of the increment for which it is called. In addition, it must provide the material Jacobian matrix $\boldsymbol{Q}_1'$ to the ABAQUS main program.

The analyzed laminate plate is simply supported around all edges and subjected to uniaxial compressive loads in the longitudinal direction only (Fig. 3). The length of the plate L is equal to 12 cm and the width of the plate W is equal to 2 cm. The laminate plate contains 4 plies with the thickness t of each ply equal to 0.1016 mm. The laminae are assumed to be perfectly bounded and no slipping occurs within the laminate. Due to the boundary conditions, the laminated plate is free to expand or contract in both x and y directions. Since the plate has no geometric imperfection in z direction, lateral deflection of the plate in z direction will not occur. Thus, the failure of the plate is due to material and not due to buckling. The stresses are uniformly distributed throughout the entire laminate plate. Hence, only one eight-node isoparametric shell elements with six degrees of freedom per node (three displacements and three rotations) is used to model the plate. The reduced integration rule together with hourglass stiffness control is employed to formulate the element stiffness matrix.[32]

In the ABAQUS program, stresses and strains in material coordinates (1, 2, 3) are calculated at each incremental step, and are evaluated by the failure criteria to determine both the occurrence of failure and the mode of failure. Mechanical properties of each lamina in the damaged area are reduced, according to proper degradation models. Stresses and strains are then recalculated to determine any additional damage as a result of stress redistribution at the same load. This procedure continues until no additional damage is found. Then, the next increment of load is pursued. The final collapse load is determined when the composite plates cannot sustain any additional load.

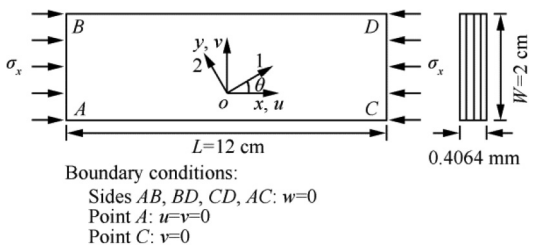

Fig. 3 Geometry and boundary conditions of composite laminates.

In order to verify the proposed nonlinear failure analysis model, numerical results generated from the model are compared with the test data of Boron/Epoxy composites.[14] The material properties of Boron/Epoxy composites used in the analysis are $E_{11e} = 207$ GPa, $E_{11pt} = E_{11pc} = 180$ GPa, $E_{22e} = 21.2$ GPa, $E_{22pt} = E_{22pc} = 15.9$ GPa, $E_{22f} = -33.12$ GPa, $G_{12} = 7.25$ GPa, $\upsilon_{12} = 0.3$, $S_{66} = 20.61 - 20\exp(-\gamma_{12}/0.00337)$ GPa^{-3} (variable), or $S_{66} = 15.20$ GPa^{-3} (constant), $X_{yt} = 828$ MPa, $X_{yc} = -1346$ MPa, $Y_{yt} = 57.9$ MPa, $Y_{yc} = -97.3$ MPa, $X_{ut} = 1370$ MPa, $X_{uc} = -2787$ MPa, $Y_{ut} = 86.3$ MPa, $Y_{uc} = -262$ MPa, $S = 128.6$ MPa. It should be noted that the shear parameter S_{66} has two types, a variable type and a constant type. The variable shear parameter is obtained by curve fitting from the pure shear test data.[15]

4.2. Verification of the proposed nonlinear constitutive model

It is necessary to assure that the proposed constitutive model can correctly simulate the stress-strain relations in the principal directions and in a pure shear of a lamina before it is utilized to predict the mechanical behavior and failure stresses of entire composite laminates under various loadings. Fig. 4 shows the numerical results for a single lamina subjected to pure shear loading against the experimental data.[14] It is

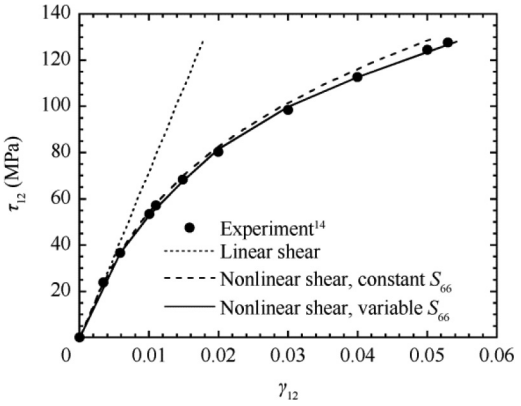

Fig. 4 Pure shear stress-strain curves for Boron/Epoxy lamina.

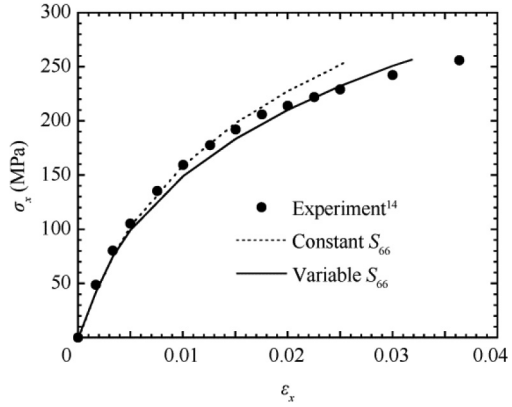

Fig. 5 Uniaxial tensile stress-strain curves for $[\pm 45]_s$ Boron/Epoxy laminate.

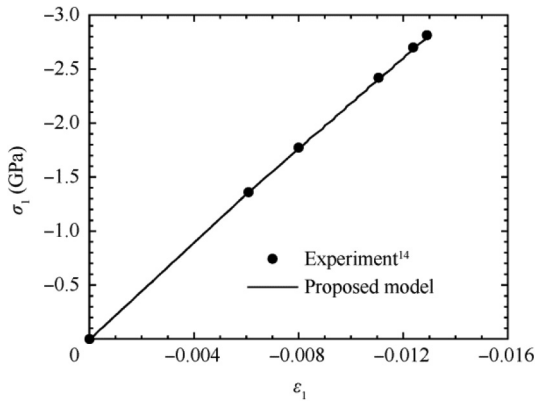

Fig. 6 Longitudinal compressive stress-strain curves for Boron/Epoxy lamina.

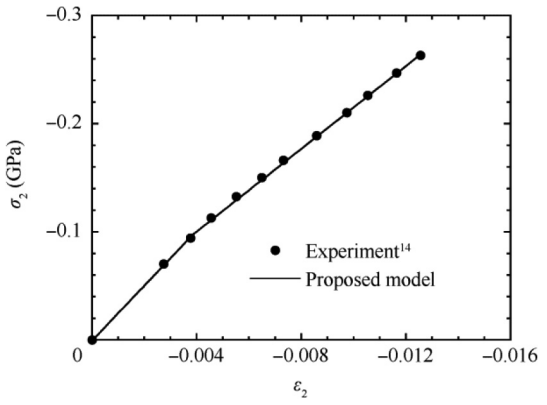

Fig. 7 Transverse compressive stress-strain curves for Boron/Epoxy lamina.

obvious that the shear stress-strain curve simulated by the proposed constitutive model with the variable S_{66} model agrees with the test data well and is much better than those with the linear shear model ($S_{66} = 0$) and the nonlinear shear model with S_{66} being constant.

The results simulated by the variable S_{66} model and the constant S_{66} model for a $[\pm 45]_s$ laminate subjected to uniaxial tension loading against the experimental data[14] are shown in Fig. 5. It can be seen that the result simulated by the proposed nonlinear shear model with the variable S_{66} exhibits better fit with the test data than that simulated by the nonlinear shear model with the constant S_{66}.

Figs. 6 and 7 illustrate the numerical results for a single lamina subjected to uniaxial longitudinal compressive loading and uniaxial transverse compressive loading against the experimental data.[14] It can be seen that the proposed elastic-plastic behavior in the longitudinal direction and transverse direction of the lamina exhibit quite good correlation with the experimental data. As a result, the proposed material model with the variable S_{66} is proved to model the nonlinear behavior of composite laminates adequately.

4.3. Comparisons among various matrix post failure modes

The load-deformation behavior of a composite laminate is greatly affected by the stress-strain behavior of individual layers within the laminate, and the ultimate strength of a composite laminate is greatly controlled by the post-damage mode of damaged lamina within the laminate. In order to verify that the proposed post-damage mode in the transverse direction of the lamina is suitable, three idealized post failure modes, brittle, ductile and degrading modes, are taken into account. Fig. 8 shows the uniaxial compressive stress-strain curves predicted by various matrix post failure modes for a $[\pm 20]_s$ angle ply laminate against the experimental data.[14] The ultimate loads predicted by the brittle mode and the degrading mode are exactly the same and equal to 0.82 GPa, which is close to the experimental data 0.75 GPa. For the ductile mode, the predicted ultimate load is significantly overestimated and is misleading.

Fig. 9 shows the uniaxial compressive stress–strain curves predicted by various matrix post failure modes for a $[\pm 30]_s$ angle ply laminate against the experimental data.[14] The ultimate load predicted by the degrading mode is 0.36 GPa, which is close to the experimental data 0.30 GPa. In the case of the brittle mode, instability exists in the fiber direction immediately after the failure of the lamina occurs. As the result, the compressive strain in the laminate is suddenly and significantly increased, which is contradictory to the experimental data. When the stress redistribution in the laminate is completed,

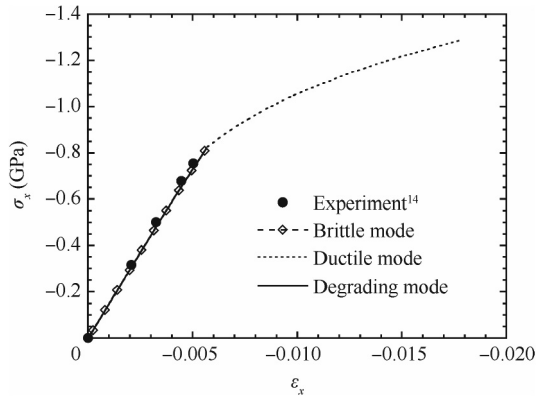

Fig. 8 Uniaxial compressive stress-strain curves predicted by various matrix post failure modes for $[\pm 20]_s$ laminate.

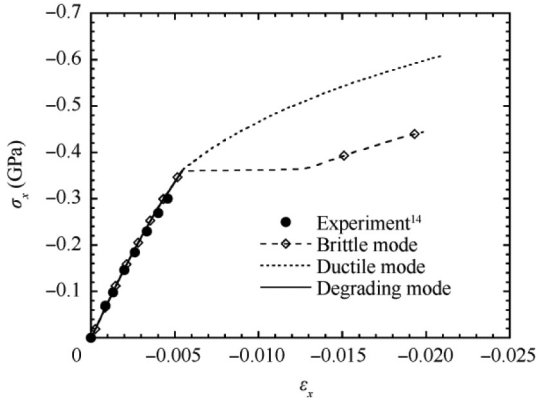

Fig. 9 Uniaxial compressive stress-strain curves predicted by various matrix post failure modes for $[\pm 30]_s$ laminate.

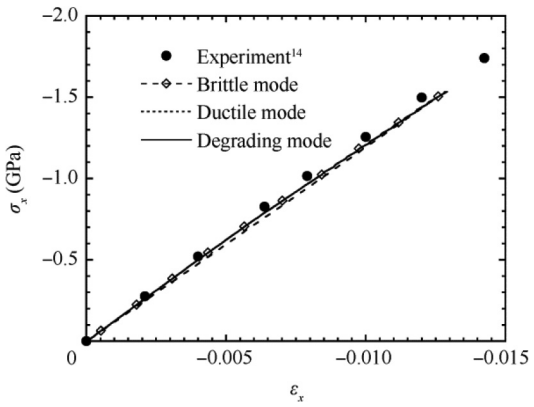

Fig. 10 Uniaxial compressive stress-strain curves predicted by various matrix post failure modes for $[0/90]_s$ laminate.

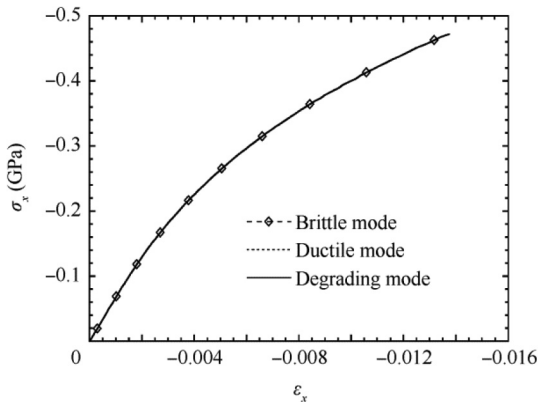

Fig. 11 Uniaxial compressive stress-strain curves predicted by various matrix post failure modes for $[15/-75]_s$ laminate.

the stress in the laminate starts to increase again, and the predicted ultimate load is 0.44 GPa, which is overestimated. For the ductile mode, the predicted ultimate load is again significantly overestimated. Hence, it is appropriate and justified to use the degrading mode to model the post failure of a lamina.

Fig. 10 shows the uniaxial compressive stress-strain curves predicted by various matrix post failure modes for a $[0/90]_s$ cross ply laminate against the experimental data.[14] While the ultimate load predicted by the brittle mode is 1.50 GPa, the ultimate loads predicted by the ductile mode and by the degrading mode are the same and equal to 1.54 GPa. It can be seen that all these predicted ultimate loads are close to the experimental data 1.74 GPa.

Figs. 11–13 show the uniaxial compressive stress-strain curves predicted by various matrix post failure modes for $[15/75]_s$, $[30/60]_s$ and $[\pm 45]_s$ cross ply laminates. Since there are no experimental data to compare, we can only see the trends. It can be observed that the predicted stress-strain curves as well as the ultimate loads with different post failure modes are exactly the same for all these three cross ply laminates. In the case of the laminates with a $[\theta/\theta - 90]_s$ cross ply layup, as the fiber angles are more deviated from 0° and 90°, the stress-strain curves of the laminates exhibit more nonlinear behavior. This is due to the nonlinear in-plane shear effect. In addition, as the fiber angles are more deviated from 0° and 90°, the ultimate loads of the laminates become lower.

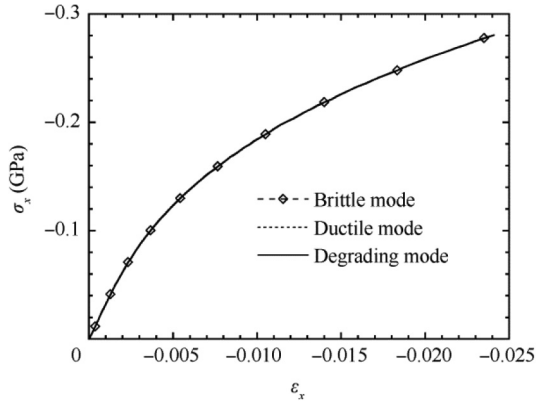

Fig. 12 Uniaxial compressive stress-strain curves predicted by various matrix post failure modes for $[30/-60]_s$ laminate.

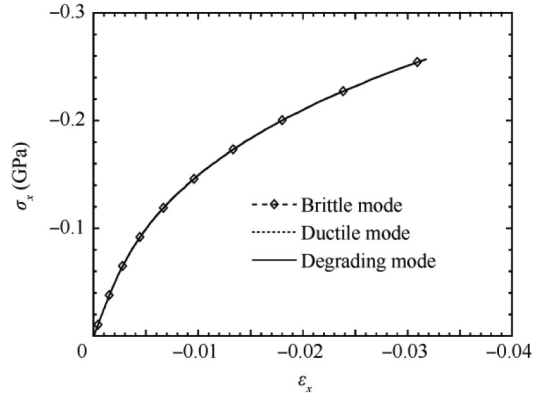

Fig. 13 Uniaxial compressive stress-strain curves predicted by various matrix post failure modes for $[\pm 45]_s$ laminate.

4.4. Comparisons among various failure criteria

The Tsai-Wu failure criterion[23] is the most popular failure criterion for composite laminate and has been extensively used in the literature on this topic. As mentioned previously, with the Tsai-Wu failure criterion, the failure stress of fiber in a lamina may exceed the strength of the material in the case of symmetric angle-ply laminates with a small fiber angle subjected to off-axis tension.[28,29] Hence, it is replaced by the mixed failure criterion, i.e., the Tsai-Wu failure criterion combined with the maximum stress criterion. In this section, the mixed failure criterion is compared with other popular criteria such as the Rotem criterion[27], the Edge criterion[26] and the Chang criterion[25] against the experimental data.[14]

Fig. 14 shows the uniaxial compressive stress-strain curves predicted by various failure criteria for a $[\pm 20]_s$ angle ply laminate against the experimental data.[14] The predicted failure loads are 818 MPa for the Rotem criterion, 775 MPa for the Edge criterion, 810 MPa for the Chang criterion and 818 GPa for the mixed criterion and the experimental failure load is 755 MPa (see Table 1). All the failure loads and the stiffnesses of the laminate predicted by the four criteria are reasonably close to the experimental data.

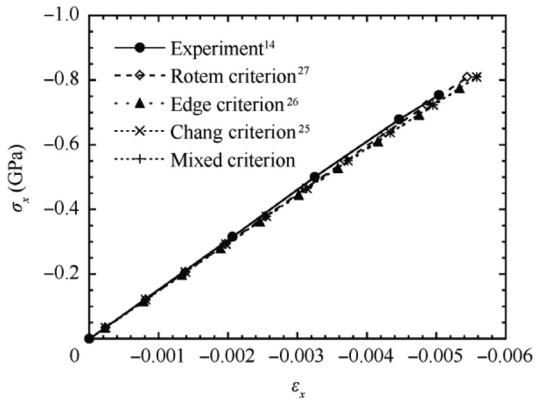

Fig. 14 Uniaxial compressive stress-strain curves predicted by various failure criterion for $[\pm 20]_s$ laminate.

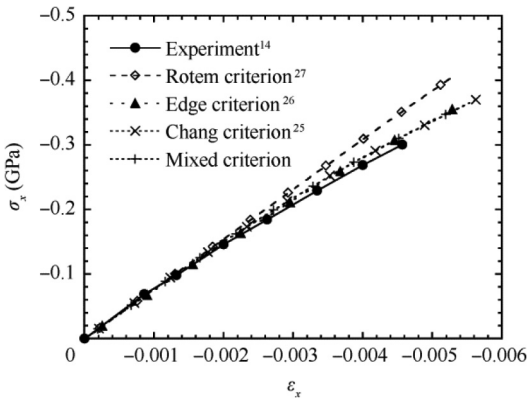

Fig. 15 Uniaxial compressive stress-strain curves predicted by various failure criteria for $[\pm 30]_s$ laminate.

Fig. 15 shows the uniaxial compressive stress-strain curves predicted by various failure criteria for a $[\pm 30]_s$ angle ply laminate against the experimental data.[14] The predicted failure loads are 406 MPa for the Rotem criterion, 355 MPa for the Edge criterion, 370 MPa for the Chang criterion and 362 MPa for the mixed criterion, and the experimental failure load is 300 MPa (see Table 1). It can be seen that the Rotem criterion overestimates the stiffness and the failure load of the laminate as compared to the other three criteria. Although, the failure loads of the laminate predicted by the other three criteria are also higher than the experimental data, the stiffnesses of the laminate predicted by the other three criteria are acceptable.

Fig. 16 shows the uniaxial compressive stress-strain curves predicted by various failure criteria for a $[\pm 60]_s$ angle ply laminate against the experimental data[14]. The predicted failure loads are 226 MPa for the Rotem criterion, 229 MPa for the Edge criterion, 249 MPa for the Chang criterion and 249 MPa for the mixed criterion, and the experimental failure load is 389 GPa (see Table 1). Although, the failure loads of the laminate predicted by all criteria are significantly underestimated as compared to the experimental data, the stress-strain curve predicted by the Rotem criterion still deviates from those predicted by the other three criteria.

Fig. 17 shows the uniaxial compressive stress-strain curves predicted by various failure criteria for a $[0/90]_s$ cross ply laminate against the experimental data.[14] The predicted failure loads are 1503 MPa for the Rotem criterion, 1503 MPa for the Edge criterion, 1535 MPa for the Chang criterion and 1535 MPa for the mixed criterion, and the experimental failure load is 1740 MPa (see Table 1). Again all the failure loads and the stiffnesses of the laminate predicted by the four criteria are reasonably close to the experimental data.

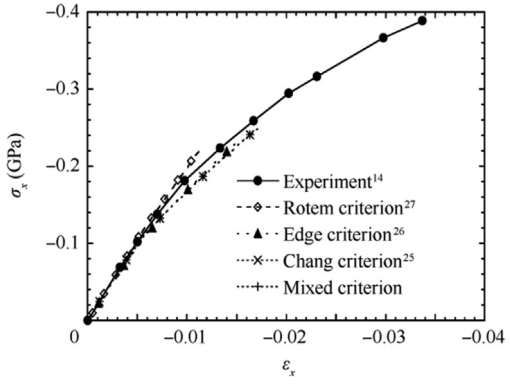

Fig. 16 Uniaxial compressive stress-strain curves predicted by various failure criteria for $[\pm 60]_s$ laminate.

Fig. 18 shows the uniaxial compressive failure stresses σ_{xf} predicted by various failure criteria for $[\pm\theta]_s$ angle ply laminates against the experimental data.[14] Fig. 19 shows the normalized material failure stresses predicted by the various failure criteria for $[\pm\theta]_s$ angle ply laminates subjected to uniaxial compressive loading. It can be observed that the failure stress σ_{xf} and the normalized failure stresses predicted by the Tsai-Wu failure criterion and the mixed failure criterion are almost the same with only a small discrepancy in the neighborhood of the angle $\theta = 45^\circ$. It should be noted that around the region $\theta = 45^\circ$, the predicted normalized failure stress $(\tau_{12f})_n$ of the Tsai-Wu failure criterion exceeds the value of 1 (see Fig. 19 (a)), which is unreasonable and unlikely to occur. This is the

Table 1 Ultimate loads predicted by the various model versus the experimental data.

Laminate	Experimental value (MPa)[14]	Rotem criterion[27]		Edge criterion[26]		Chang criterion[25]		Mixed criterion	
		Value (MPa)	Error (%)	Value (MPa)	Error (%)	Value (MPa)	Error (%)	Value (MPa)	Error (%)
$[\pm 20]_s$	755	818	8.3	775	2.6	810	7.3	818	8.3
$[\pm 30]_s$	300	406	35.3	355	18.3	370	23.3	362	20.7
$[\pm 60]_s$	389	226	41.9	229	41.1	249	36.0	249	36.0
$[0/90]_s$	1740	1503	13.6	1503	13.6	1535	11.8	1535	11.8

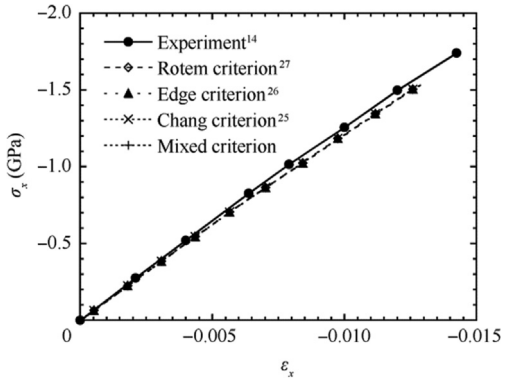

Fig. 17 Uniaxial compressive stress-strain curves predicted by various failure criteria for $[0/90]_s$ laminate.

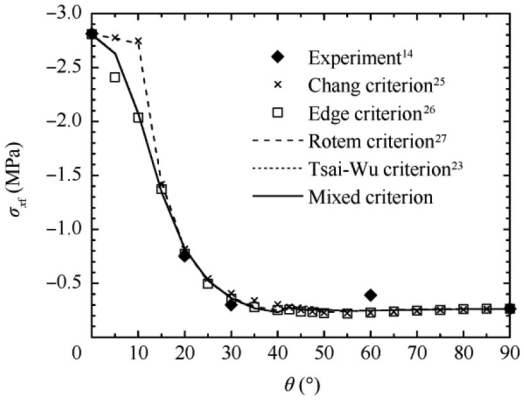

Fig. 18 Uniaxial compressive failure stresses predicted by various failure criteria for $[\pm\theta]_s$ angle ply laminates.

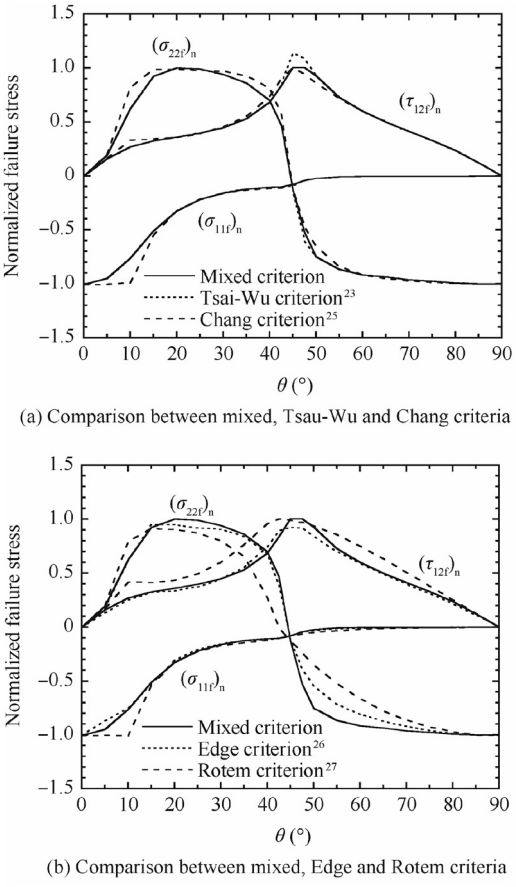

Fig. 19 Normalized material failure stresses predicted by various failure criteria for $[\pm\theta]_s$ angle ply laminates subjected to uniaxial compressive loading.

reason why the authors propose a mixed failure criterion for the cases of laminates subjected to uniaxial tensile loads.[28,29]

Comparing the Chang failure criterion with the mixed criterion, we can determine that the failure stress σ_{xf} and the normalized failure stresses predicted with these two criteria are about the same except in the region $0^\circ \leqslant \theta \leqslant 15^\circ$. This is because the Chang failure criterion does not consider the joint effect due to axial stress, transverse stress and in-plane shear stress acting simultaneously. When $0^\circ \leqslant \theta \leqslant 10^\circ$. we can see that the failure of the angle ply laminate is due to axial failure stress $(\sigma_{11f})_n$ for the Chang criterion (see Fig. 19(a)). If the joint effect of axial stress, transverse stress and in-plane shear stress is considered, such as the Tsai-Wu failure criterion, the predicted failure stress σ_{xf} and the normalized failure stresses (in absolute values) will not be so high within the $0^\circ \leqslant \theta \leqslant 15^\circ$ region.

In the case of the Edge criterion, it can be seen that its predicted failure stress σ_{xf} is usually lower than those predicted by other criteria (see Fig. 18). The reason for this is the fact that its predicted stresses σ_1, σ_2 and τ_{12} are smaller (in absolute value) than those predicted by other criteria, which can be clearly seen in Fig. 19(b).

In the case of the Rotem criterion, the predicted failure stress σ_{xf} is usually higher than those predicted by other failure criteria when $\theta \leqslant 45^\circ$ and lower than those predicted by other failure criteria when $\theta \geqslant 45^\circ$ (see Fig. 18). When $0^\circ \leqslant \theta \leqslant 15^\circ$, the Rotem criterion, like the Chang criterion, does not consider the joint effect due to axial stress, transverse stress and in-plane shear stress acting simultaneously. Hence, it has the similar trend as the Chang criterion. When $15^\circ \leqslant \theta \leqslant 80^\circ$,the predicted transverse stress σ_2 by the Rotem criterion is lower than that by mixed criterion, and the predicted in-plane shear stress τ_{12} by the Rotem criterion is higher than that by mixed criterion (see Fig. 19(b)). This is due to the Rotem model treating the in-plane shear as having linear behavior. Therefore, it overestimates the in-plane shear stress. After the failure criterion is employed, the transverse stress is then underestimated.

5. Conclusions

This paper proposes a material constitutive model for the analysis of composite laminates subjected to uniaxial compressive loads. The main outcomes of the model contain three parts: (A) nonlinear constitutive model, (B) mixed failure criterion, and (C) post-damage mode. In the nonlinear constitutive model, the fiber and matrix are simulated by elastic-plastic behavior and the in-plane shear is simulated by nonlinear behavior with a variable shear parameter. The mixed failure criterion is composed of the Tsai-Wu failure criterion and the maximum stress criterion, which can avoid the overestimation of stresses predicted by the Tsai-Wu failure criterion. In the post-damage regions, the fiber and the in-plane shear are

simulated by a brittle mode, and the matrix is simulated by a degrading mode. The validity of the constitutive model has been verified against the experimental data[14] and reasonable accuracy has been achieved.

The proposed constitutive model has been compared with other popular failure criteria for $[\pm\theta]_s$ angle ply laminates subjected to uniaxial compressive loads. In the case of the Chang criterion, the predicted failure stress σ_{xf} is usually higher than the mixed criterion and the Tsai-Wu criterion when $0^\circ \leqslant \theta \leqslant 15^\circ$. In the case of the Edge criterion, the predicted failure stress σ_{xf} is usually lower than the mixed criterion and the Tsai-Wu criterion. In the case of the Rotem criterion, the predicted failure stress σ_{xf} is usually higher than those predicted by the mixed criterion and the Tsai-Wu criterion when $\theta \leqslant 45^\circ$ and lower than those predicted by the mixed criterion and the Tsai-Wu criterion when $\theta \geqslant 45^\circ$.

References

1. Chang FK, Chang KY. A progressive damage model for laminated composites containing stress concentrations. *J Compos Mater* 1987;**21**(9):834–55.
2. Hinton MJ, Soden PD. Predicting failure in composite laminates: Background to the exercise. *Compos Sci Technol* 1998;**58**(7):1001–10.
3. Sun CT, Tao JX. Prediction of failure envelopes and stress/strain behaviour of composites laminates. *Compos Sci Technol* 1998;**58**(7):1125–36.
4. Spootswood MS, Palazotto AN. Progressive failure analysis of a composite shell. *Compos Struct* 2001;**53**(1):117–31.
5. Hu H-T, Yang C-H, Lin F-M. Buckling analyses of composite laminate skew plates with material nonlinearity. *Compos B Eng* 2006;**37**(1):26–36.
6. Tay TE, Liu G, Tan VBC, Sun XS, Pham DC. Progressive failure analysis of composites. *J Compos Mater* 2008;**42**(18):1921–66.
7. Pham DC, Sun XS, Tan VBC, Chen B, Tay TE. Progressive failure analysis of scaled double-notched carbon/epoxy composite laminates. *Int J Damage Mech* 2012;**21**(8):1154–85.
8. Turan K, Kaman MO, Gur M. Progressive failure analysis of laminated composite plates with two serial pinned joints. *Mech Adv Mater Struct* 2015;**22**(10):839–49.
9. Liu PF, Yang YH, Gu ZP, Zheng JY. Finite element analysis of progressive failure and strain localization of carbon fiber/epoxy composite laminates by ABAQUS. *Appl Compos Mater* 2015;**22**(6):711–31.
10. Kozlov MV, Sheshenin SV. Modeling the progressive failure of laminated composites. *Mech Compos Mater* 2016;**51**(6):695–706.
11. Namdar Ö, Darendeliler H. Buckling, postbuckling and progressive failure analyses of composite laminated plates under compressive loading. *Compos B Eng* 2017;**120**:143–51.
12. Zhou S, Sun Y, Chen BY, Tay TE. Progressive damage simulation of open-hole composite laminates under compression based on different failure criteria. *J Compos Mater* 2017;**51**(9):1239–51.
13. Hahn HT, Tsai SW. Nonlinear elastic behavior of unidirectional composite laminae. *J Compos Mater* 1973;**7**(1):102–18.
14. Petit PH, Waddoups ME. A method of predicting the nonlinear behavior of laminated composites. *J Compos Mater* 1969;**3**(1):2–19.
15. Jones RM, Morgan HS. Analysis of nonlinear stress-strain behavior of fiber-reinforced composite materials. *AIAA J* 1977;**15**(12):1669–76.
16. Bogetti TA, Hoppel CPR, Harik VM, Newill JF, Burns BP. Predicting the nonlinear response and progressive failure of composite laminates. *Compos Sci Technol* 2004;**64**(3–4):329–42.
17. Griffin OH, Kamat MP, Herakovich CT. Three-dimensional inelastic finite element analysis of laminated composites. *J Compos Mater* 1981;**15**(6):543–60.
18. Kenaga D, Doyle JF, Sun CT. The characterization of boron/aluminum composite in the nonlinear range as an orthotropic elastic-plastic material. *J Compos Mater* 1987;**21**(6):516–31.
19. Vaziri R, Olson MD, Anderson DL. A plasticity-based constitutive model for fibre-reinforced composite laminates. *J Compos Mater* 1991;**25**(5):512–35.
20. Allen H, Harris CE, Groves SE. A thermomechanical constitutive theory for elastic composites with distributed damage—I, Theoretical development. *Int J Solids Struct* 1987;**23**(9):1301–18.
21. Rowlands RE. Strength (failure) theories and their experimental correlation. In: Sih GC, Skudra AM, editors. *Failure Mechanics of Composites*. Amsterdam: Elsevier; 1985. p. 71–125.
22. Hoffman O. The brittle strength of orthotropic materials. *J Compos Mater* 1967;**1**(2):200–6.
23. Tsai SW, Wu EM. A general theory of strength for anisotropic materials. *J Compos Mater* 1971;**5**(1):58–80.
24. Lee JD. Three dimensional finite element analysis of damage accumulation in composite laminate. *Comput Struct* 1982;**15**(3):335–50.
25. Chang FK, Lessard LB. Damage tolerance of laminated composite containing an open hole and subjected to compressive loadings: Part I—Analysis. *J Compos Mater* 1991;**25**(1):2–43.
26. Edge EC. Stress based grant-sanders method for predicting failure of composite laminates. *Compos Sci Technol* 1998;**58**(7):1033–41.
27. Rotem A. Prediction of laminate failure with the Rotem failure criterion. *Compos Sci Technol* 1998;**58**(7):1083–94.
28. Lin W-P, Hu H-T. Nonlinear analysis of fiber-reinforced composite laminates subjected to uniaxial tensile load. *J Compos Mater* 2002;**36**(12):1429–50.
29. Lin W-P, Hu H-T. Parametric study on the failure of fiber-reinforced composite laminates under biaxial tensile load. *J Compos Mater* 2002;**36**(12):1481–504.
30. Hu H-T, Lin W-P, Tu F-T. Failure analysis of fiber-reinforced composite laminates subjected to biaxial loads. *Compos B Eng* 2015;**83**:153–65.
31. Zhu H, Sankar BV. Evaluation of failure criteria for fiber composites using finite element micromechanics. *J Compos Mater* 1998;**32**(8):766–82.
32. Dassault Systèmes Corporation. SIMULIA ABAQUS analysis user's manuals, Theory manuals and example problems manuals. Pairs: Dassault Systèmes Corporation; 2018
33. Mindlin RD. Influence of rotatory inertia and shear on flexural motions of isotropic elastic plate. *J Appl Mech* 1951;**18**:31–8.
34. Narayanaswami R, Adelman HM. Evaluation of the tensor polynomial and Hoffman strength theories for composite materials. *J Compos Mater* 1977;**11**(4):366–77.
35. Hu H-T. Buckling analyses of fiber composite laminate shells with material nonlinearity. *J Compos Technol Res* 1993;**15**(3):202–8.
36. Hu H-T. Buckling analyses of fiber composite laminate plates with material nonlinearity. *Finite Elem Anal Des* 1995;**19**(3):169–79.